Jilin Daxue Xuebao (Gongxueban)/Journal of Jilin University (Engineering and Technology Edition)
ISSN: 1671-5497
E-Publication: Online Open Access
Vol: 43 Issue: 03-2024
DOI: 10.5281/zenodo.10792464

EFFECT OF TEMPERATURE (1300, 1350, 1400, 1450 AND 1500 K) ON THE CRYSTALLINE PARAMETER AND ON THE ENERGY OF FORMATION OF VACANT SITES IN Ti-xAl (x=50, 55, 60%)

ALAIN SECOND DZABANA HONGUELET
Faculty of Science and Technology, Marien Ngouabi University, Congo Brazzaville.
Research Group on the Physical and Chemical Properties of Materials, Congo Brazzaville.
Association Alpha Sciences Beta Technologies, Congo Brazzaville.
*Corresponding Author Email: second_alain@yahoo.fr

DIMITRI HERMANN N'GOYA DHA TABATSIA
Faculty of Science and Technology, Marien Ngouabi University, Congo Brazzaville.
Research Group on the Physical and Chemical Properties of Materials, Congo Brazzaville.

RONOLVIE BITHO ONDONGO
Faculty of Science and Technology, Marien Ngouabi University, Congo Brazzaville.
Research Group on the Physical and Chemical Properties of Materials, Congo Brazzaville.

EARVIN LOUMBANDZILA
Faculty of Science and Technology, Marien Ngouabi University, Congo Brazzaville.
Research Group on the Physical and Chemical Properties of Materials, Congo Brazzaville.
Association Alpha Sciences Beta Technologies, Congo Brazzaville.

TIMOTHÉE NSONGO
Faculty of Science and Technology, Marien Ngouabi University, Congo Brazzaville.
Research Group on the Physical and Chemical Properties of Materials, Congo Brazzaville.
Center for Geological and Mining Research, Congo Brazzaville.

Abstract

In this work, we have studied the vacancy formation energy of Ti-Al alloy of structure B2 with size 10*10*10 for aluminum percentages of 50, 55 and 60% under the influence of temperature at 1300, 1350, 1400, 1450 and 1500K using the Modified Emmbedded Atom Method (MEAM) under the LAMMPS version 2020 calculation code. This study has enabled us to understand the behavior of the Ti-Al alloy under different percentages in terms of total energy, vacancy formation energy and crystalline parameter. For each of these physical quantities, we have shown that the total energy decreases with temperature; this is also verified for the percentage, with the lowest energy obtained for the Ti-60% Al structure at 1300K of the order of -8678.4149mjmm^2. The Ti-50%Al alloy has positive energies of formation, so this structure forms whatever the chosen operating temperature, which is not the case for Ti-55%Al. At 1350 K, we observed an inversion in the mesh parameter behavior of the Ti-60%Al alloy, which we attributed to the phase change around 1350K. At 1400K, we observed a reversal in the behavior of total energy.

Keywords: LAMMPS, Formation Energy, Titanium Alloy, MEAM, Vacant Sites, Molecular Dynamics.

1. INTRODUCTION

In the transport sector, the search for performance and weight reduction are often criteria sought by manufacturers. These criteria are mainly determined by the choice of materials. Chemical composition, thermomechanical and thermal treatments, and surface

Jilin Daxue Xuebao (Gongxueban)/Journal of Jilin University (Engineering and Technology Edition)
ISSN: 1671-5497
E-Publication: Online Open Access
Vol: 43 Issue: 03-2024
DOI: 10.5281/zenodo.10792464

treatments all have a strong influence on a material's ability to withstand mechanical stress and the environment in which it is exposed.

Titanium alloys can meet the requirements of an industry focused on transportation, such as aviation and shipping. They offer a good compromise between mechanical properties and density, and have good corrosion resistance.

A well-known alloy, widely used in the aerospace and biomedical sectors, is Ti-6Al-4V with its two-phase α+β microstructure. However, this alloy is limited in terms of mechanical properties for use in marine applications.

In order to achieve higher mechanical properties, it is preferable to use β-metastable titanium alloys, which have an excellent mechanical strength! Density ratio, higher than that of Ti-6Al-4V alloys, and are highly resistant to corrosion.

Another important criterion for a company is the cost of the material up to the production of the part, which must be economically viable for the company. The choice of titanium and its alloys proves expensive at the outset, but their excellent properties give them a sufficiently long service life for the industrialist to select this material [1].

Alloys based on the intermetallic compound TiAl have been attracting growing interest from the scientific community in recent years, with a view to structural applications in the aerospace and automotive sectors. Thanks to their properties. They can also be high-potential candidates and play a key role in military applications (ballistics, armor) [2]. TiAL alloys are intermetallics with a long-range ordered crystallographic structure. The interatomic bonds are not only metallic, but also covalent, giving them high strength but also a certain brittleness. The main characteristic of these alloys is to combine a low density (≈4 g/cm3), of the order of half that of superalloys (≈ 8 g/cm3), with high mechanical strength at high temperatures, and good resistance to oxidation. These properties give these materials great potential in high-temperature industrial, aerospace and automotive applications. [2]

At the Faculty of Science and Technology, the Groupe de Recherche sur les Propriétés Physiques et Chimiques des Matériaux (Physical and Chemical Properties of Materials Research Group) has been making Ti-Al an exciting subject for some years now. Professor Timothée NSONGO has studied the order-disorder transformation of the Ti-Al binary alloy system by numerical simulation using the EAM inserted atom method. The main aim of his thesis was to determine the influence of mesh constant and composition on the type of order-disorder transformation and the order process in alloys.

Ti-Al alloys are currently being extensively studied for their mechanical and structural properties, but defects such as vacancies can dramatically alter the properties of these materials.

The B2-type Ti-Al structure is metastable, and it remains interesting to be able to study it in order to produce other alloys that are stable at favorable temperatures, thanks to the use of vacant sites.

Jilin Daxue Xuebao (Gongxueban)/Journal of Jilin University (Engineering and Technology Edition)
ISSN: 1671-5497
E-Publication: Online Open Access
Vol: 43 Issue: 03-2024
DOI: 10.5281/zenodo.10792464

We have studied the vacancy formation energy of Ti-Al alloy of B2 structure of size 10*10*10 for aluminum percentages of 50, 55 and 60% under the influence of temperature of 1300,1350, 1400,1450 and 1500K using the Modified Embedded Atom Method (MEAM) under LAMMPS calculation code version 2020. This study is carried out to understand the behavior of Ti-AL alloy under different percentages in terms of total energy, vacancy formation energy, crystalline parameter.

The aim of this work is therefore to study the Ti-Al alloy system in B2 structure at different temperatures (1300, 1350, 1400 and 1500 K) for each of the aluminum atomic percentages of 50, 55 and 60%, in order to determine the influence of this composition and temperature on the lattice parameter and to determine its vacancy formation energy.

2. METHODOLOGIES

Numerical methods are valuable tools for studying materials at the atomic scale. However, it is essential to choose a tool that is well suited to the problem. Each type of method has its own temporal and spatial limitations. In addition, some problems may require multi-scale methods involving different combinations of methods. We can also note that each of these methods is potentially limited by the physical components of the computers on which they are run. Thus, for the purposes of this thesis, we have chosen to work with molecular dynamics. As its name suggests, this allows us to study the dynamics of molecules or atoms.

2.1 Molecular dynamics

Molecular dynamics simulations are highly effective for studying the temperature behavior of a material. Moreover, anharmonic and collective effects can be taken into account without additional assumptions. Molecular dynamics provides access to both the temporal evolution of a system and the measurement of its thermodynamic quantities. It is therefore the method of choice for studying the Ti-Al phase diagram.

2.1.1 Principle of molecular dynamics

Classical molecular dynamics (MD) is based on Newtonian mechanics: the properties of a set of atoms (e.g. thermal conductivity) or particles are determined by studying the trajectory of each particle over time. To do this, the laws of classical mechanics are applied to atoms, which are treated as point masses. The classical equations of motion are thus solved simultaneously for all atoms in a system:

$$\overrightarrow{f_i} = m_i \overrightarrow{a_i} \qquad \textbf{Equation (1)}$$

Where $\overrightarrow{f_i}$ is the sum of the forces acting on atom i, m_i its mass and $\overrightarrow{a_i}$ its acceleration. The interaction forces (or the potentials from which they derive : $F = -gradV$where V is a potential and F a force) can be obtained from the first principles of quantum mechanics.

This is referred to as ab-initio DM, but more often than not it is derived from an empirically fixed potential, and is referred to as classical DM. In practice, we prefer to define interactions between atoms on the basis of potentials [3].

Jilin Daxue Xuebao (Gongxueban)/Journal of Jilin University (Engineering and Technology Edition)
ISSN: 1671-5497
E-Publication: Online Open Access
Vol: 43 Issue: 03-2024
DOI: 10.5281/zenodo.10792464

The equations of motion must be integrated numerically, choosing a finite time step δt and approximating the differential equations by finite difference equations. From these calculations, the computer predicts the new positions, velocities and forces of all particles at time t+δt. In this way, we can trace the behavior of a material: for example, the movement and rearrangement of atoms/defects....

The input data for a molecular dynamics calculation are therefore:

a set of atoms, representing in our case the system to be studied;

interatomic potentials, the determination of which requires prior study;

a series of constraints imposed by the external environment (pressure, temperature, etc.).

2.1.2 Time evolution algorithm

The choice of an algorithm for integrating equations of motion is guided by its speed of execution. In other words, by the possibility of having the largest possible integration steps, while conserving the system's energy.

Molecular dynamics studies the evolution over time of a system of N interacting atoms. To do this, we integrate the equations of classical mechanics:

$$\boldsymbol{m}\frac{\boldsymbol{d^2 r\alpha}}{\boldsymbol{dt^2}} = \boldsymbol{f_\alpha} \qquad \textbf{Equation (2)}$$

Where α travels through the individual atoms. To solve these 3N differential equations, it is necessary to be able to evaluate the force experienced by each atom and then numerically integrate the differential equations.

To integrate differential equations, we use a standard equation discretization technique, with a time step δt. The smaller the δt, the more accurate the numerical integration, but the longer the calculation time. In practice, it is sufficient for δt to be small compared with the characteristic time of evolution of the system, i.e. a time over which the forces can be considered as quasi-constant.

Numerous time integration methods exist; whose error is generally polynomial in δt. The method often used in molecular dynamics is the Verlet algorithm [4].

Consider that we know the positions of all atoms at time t and t+δt. The positions at time *t* and *t - δt* are obtained by :

$$\boldsymbol{r_\alpha(t+\delta t) = 2r_\alpha(t) - r_\alpha(t-\delta t) + \frac{f_\alpha(t)}{m}\delta t^2} \qquad \textbf{Equation (3)}$$

and speeds by :

$$\boldsymbol{V_\alpha(t) = \frac{r_\alpha(t+\delta t) - r_\alpha(t-\delta t)}{2\delta t}} \qquad \textbf{Equation (4)}$$

This is a method whose error on positions is in δt^4 . It's not the most accurate method available, but it does have a number of advantages. It's a simple method, involving only the two time steps preceding the one you wish to calculate. We therefore need to store the particle positions in memory only twice. Verlet's algorithm is numerically very stable.

Jilin Daxue Xuebao (Gongxueban)/Journal of Jilin University (Engineering and Technology Edition)
ISSN: 1671-5497
E-Publication: Online Open Access
Vol: 43 Issue: 03-2024
DOI: 10.5281/zenodo.10792464

What's more, it is invariant to time reversal, which is a fundamental property of classical mechanics, but is not respected by more precise and complex methods such as the Runge-Kunta method **[5].**

In practice, we need to choose an initial state at $t = t_0$ consisting of the position and velocity of all particles, but we also need the positions of the atoms at $t=t_0 + \delta t$. For this, we use a less precise method, but requiring only a previous time step, the Taylor algorithm:

$$\boldsymbol{r_\alpha(t+\delta t) = r_\alpha(t) + V_\alpha(t)\delta t + \frac{f_\alpha(t)}{m}\frac{\delta t^2}{2}} \qquad \textbf{Equation (5)}$$

If we choose an initial state "far away" from the state we want to simulate, the system will take a long time to reach this state, and may get stuck in a metastable state. To ensure that the initial state is not too far away, we choose, for crystalline solids, to take the initial positions on the perfect geometric structure. To initialize the velocities, we generally choose a temperature T_0 and randomly draw the velocities according to the Maxwell-Boltzmann distribution. However, the temperature of the system at equilibrium will not be T_0.

In fact, the simulated system (N particles in a box) exchanges neither energy nor particles with the outside world. We are therefore in the micro-canonical set, for which the system's energy is conserved, but not its temperature. In practice, about half the kinetic energy is converted into potential energy, so the equilibrium temperature is close to $T_0/2$.

However, we may often wish to impose a temperature or pressure on the system, i.e. to move from the canonical micro set to other statistical sets. Extensions to molecular dynamics are then necessary, introducing fictitious additional degrees of freedom. With the right choice of dynamic equations governing these additional variables, it is then possible to simulate ensembles other than the canonical micro ensemble. The most common of these are: the canonical ensemble with the Nosé method **[6,7]** and the ensemble at constant temperature and pressure with the Nosé-Andersen **[8,9]** and Parinello-Rahman **[10]** methods**.**

2.1.3 Boundary conditions

To have a realistic physical system, it's also important to treat the boundary conditions correctly, i.e. the interaction of particles with the edges of the box. Depending on the physical system we want to model, we can, among other things, decide that the atoms at the edge are fixed, or that they reflect perfectly off the walls. In our case, we want to model a macroscopic solid, made up of 2,000 atoms. For such small solids, surface effects are important, whereas we want to model the massive material.

To eliminate these surface effects, we generally use periodic boundary conditions, also known as Born-Von Kár-man conditions. These consist in imagining that the simulation box is surrounded by copies of itself. An atom exiting the box from one side therefore re-enters from the opposite side at the same speed. Similarly, an atom placed near one side of the box interacts with the image of the atom on the opposite side. In this way, we can model a system of infinite size with a reasonable number of particles. However, this principle cannot be used to simulate correlated effects on very large scales,

Jilin Daxue Xuebao (Gongxueban)/Journal of Jilin University (Engineering and Technology Edition)
ISSN: 1671-5497
E-Publication: Online Open Access
Vol: 43 Issue: 03-2024
DOI: 10.5281/zenodo.10792464

as we are then obliged to use a very large number of atoms or to change the type of boundary conditions.

2.2 Structure and interatomic potentials

2.2.1 The equilibrium phase diagram

The phase diagram used as a reference until 1989 was established by Murray in 1986 (Fig. I. 1), and was derived from a correlation between theoretical and experimental results acquired since the 1950s [**11,12]**.

In 1989, a new diagram was proposed by *Mc Cullough et al. for Ti-Al alloys containing 40-55 atomic % aluminum*. These changes are based on morphological observations of the dendrites and in situ X-ray diffraction studies of the high-temperature phases.

This revised diagram (Fig. 1) incorporates two peritectics L + β → γ and L + α → γ, and extends the α range to higher temperatures [**11,12,13]**. The same changes in the diagram, based on metallographic observations after heat treatments and on dilatometer results, have been proposed by Huang et al. **[14,15].**

These changes concern the part of the diagram above the α transus (α / α + γ transition). The low-temperature range, below the eutectoid plateau, remains unchanged.

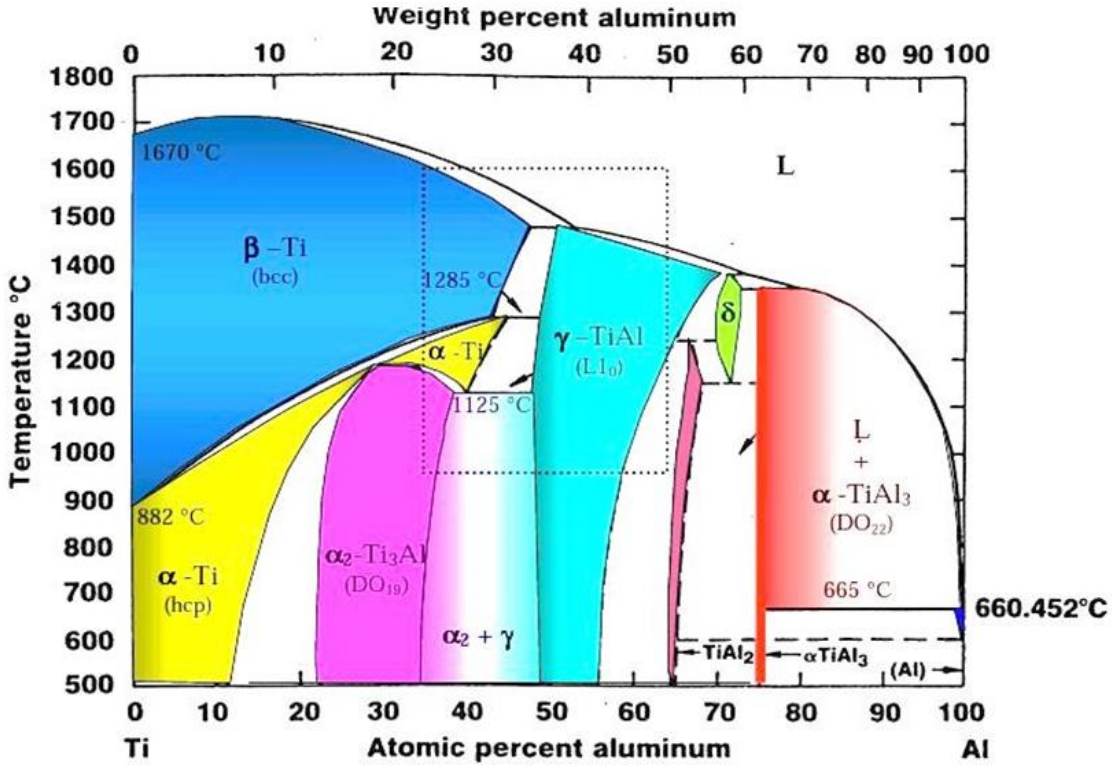

Figure 1: Ti-Al phase diagram from Murray [20].

Jilin Daxue Xuebao (Gongxueban)/Journal of Jilin University (Engineering and Technology Edition)
ISSN: 1671-5497
E-Publication: Online Open Access
Vol: 43 Issue: 03-2024
DOI: 10.5281/zenodo.10792464

The equilibrium phase diagram of the Ti-Al binary system contains eight different phases:

- L: the liquid phase,
- β-Ti (bcc) and α-Ti (hcp): two primary solid solutions of aluminum in titanium.

They are derived from the two allotropic forms of Ti. The allotropic transformation of titanium, β-Ti (bcc) → α-Ti (hcp), occurs at 882°C.

- α2-Ti3Al: intermediate, hexagonal, ordered DO19-type solid solution from the primary α-Ti phase,
- γ-TiAl: intermediate, quadratic, ordered L10-type solid solution,
- TiAl2: intermediate solid solution; quadratic (24 atoms/mesh**)**,
- δ: intermediate solid solution
- TiAl3: defined compound with non-congruent melting,
- α-Al (CFC): primary solid solution of titanium in aluminum.

The diagram also shows:

- four peritectic stages characterized by the following transformations:
  - *at 1487.5°C: β-Ti (47.70%) + L (53%) ⇔ γ-TiAl (51.2%);*
  - *at 1450.5°C: γ-TiAl (70.5%) + L (73.5%) ⇔ δ (71.5%);*
  - *at 1346.8°C: δ (73.1%) + L (80.8%) ⇔ γ-TiAl2(75%);*
  - *at 665°C: Ti3Al (75%) + L (99.75%) ⇔ α-Al (98.75%).*
- two peritectoid stages characterized by the following transformations:
  - *at 1285°C: β-Ti (%) + γ-TiAl (%) ⇔ α-Ti (%);*
  - *at 1285°C: γ-TiAl (%) + δ (%) ⇔ TiAl2 (%).*
- two eutectoid stages characterized by the following transformations:
  - *at 1150°C: δ (71.5%) ⇔ TiAl2(67.66%) + α-TiAl3(75%);*
  - *at 1125°C: α-Ti (40.36%) ⇔ α2-Ti3Al (38.75%) + γ-TiAl (50.5%).*

The main ingredient of the simulations is the description of the interaction forces between the atoms or, more generally, the knowledge of the dependence of the total energy of the system on the position of the atoms. Interaction potentials can be established with the aid of quantum mechanical electronic structure calculations.

The interatomic interaction potential is a function V ($\vec{r_1}$,$\vec{r_2}$, $\vec{r_3}$.....) of the positions of the atoms, which represents the potential energy of the system.

Jilin Daxue Xuebao (Gongxueban)/Journal of Jilin University (Engineering and Technology Edition)
ISSN: 1671-5497
E-Publication: Online Open Access
Vol: 43 Issue: 03-2024
DOI: 10.5281/zenodo.10792464

The development of such potentials is a two-stage process.

- First, the analytical form of the function is chosen (it often depends on the type of bonds involved: ionic, covalent, Van der Waals, etc.), which can be parameterized.
- The function is then adjusted according to a number of carefully chosen physical properties: cohesion energy, elasticity constants, gap formation energy, surface energies, interface energy, phonon spectrum, pressure-volume relationship... - depending on the field of application.

2.2.2 Modified embedded atom method and interatomic potential

Interatomic potentials are of vital importance for simulations that model the properties of materials. The basis for these potentials is Density Function Theory (DFT), which postulates that energy is a function of electron density. By knowing the electron density of an entire system, we can determine the potential energy of a system:

$$U=[\rho(r)] \qquad \textbf{Equation(6)}$$

$$E[\rho(r)]=Ts[\rho(r)]+J[\rho(r)]+E_{xc}[\rho(r)]+Eext[\rho(r)]+E_{ii}[\rho(r)] \qquad \textbf{Equation(7)}$$

where E is the total energy, Ts is the kinetic energy of the single particle, J is the Hartree electron-electron energy, E_{xc} is the exchange correlation function, E_{ext} is the electron-ion coulombic interaction, and E_{ii} is the ion-ion energy.

On this basis, the Embedded Atom Method (EAM) was created on the assumption that an atom can be embedded in a homogeneous electron gas and that the change in potential energy is a function of the electron density of the embedded atom, which can be approximated by an embedding function. In a crystal, however, the electron density is not homogeneous, so the EAM potential replaces the background electron density with the electron densities of individual atoms, and supplements the embedding energy with a repulsive pair potential to represent the core-core interactions of the atoms.

With a simple linear superposition of atomic electron densities as the background electron density, the EAM is governed by the following equations:

$$R_{ij}=|ri-rj| \qquad \textbf{Equation (8)}$$

$$\rho\bar{i}=\Sigma(Rij)j \qquad \textbf{Equation (9)}$$

$$U=\Sigma(\rho\bar{i})i+12\Sigma\phi(Rij)i,j \qquad \textbf{Equation (10)}$$

Where Rij is the distance between atoms i and j, ρj is the atomic electron density, ri is the position of atom i, F is the embedding function, ρi are the electron densities, and ϕ is the peer interaction potential.

However, EAM does not do an excellent job of simulating materials with significant directional binding, which includes most metals. In order to simulate metals correctly, the modified embedded atom method was created, which allows the background electron density to depend on the local environment instead of assuming a linear superposition. The equation governing the potential energy is

Jilin Daxue Xuebao (Gongxueban)/Journal of Jilin University (Engineering and Technology Edition)
ISSN: 1671-5497
E-Publication: Online Open Access
Vol: 43 Issue: 03-2024
DOI: 10.5281/zenodo.10792464

$$U=\Sigma(\rho\bar{i})_i +12\Sigma\phi_{ij}\,(R_{ij})S(R_{ij})_i\,,\ j\neq i \qquad \textbf{Equation(11)}$$

The main difference between the potential energy equation for EAM and MEAM is the inclusion of S, which is the radial screen.

For a MEAM interatomic potential that describes the relationship for alloys with two or more components, each individual component needs 13 individual adjustable parameters. In addition, each binary interaction requires at least 14 adjustable parameters. These parameters are used in the calculation of the potential energy described in equation 8 and govern the forces acting on the atoms. These parameters are listed below in Tables 2.

2.2.3 Thermodynamic assemblies

Thermodynamic assemblies are used to fix one or more properties of the system under study (volume, temperature, pressure, enthalpy). There are several thermodynamic assemblies used in molecular dynamics: the microcanonical set, the canonical assembly and the isothermal-isobaric assembly. In essence, DM explores the NVE microcanonical assembly, for which the number of atoms (N), the volume studied (V) and the energy of the system (E) are fixed. For the other assemblies (canonical NVT, isothermal-isobaric NPT), we have to modify Newton's equations.

The following assemblies are used:

- *The NVE set (Number of Atoms - Volume - Energy): this set is not the natural set for experiments. It is used to quantify heat transfer;*
- *The NPH set (Number of atoms - Pressure - Enthalpy): used to relax structures;*
- *The NVT set (Number of atoms - Volume - Temperature).*

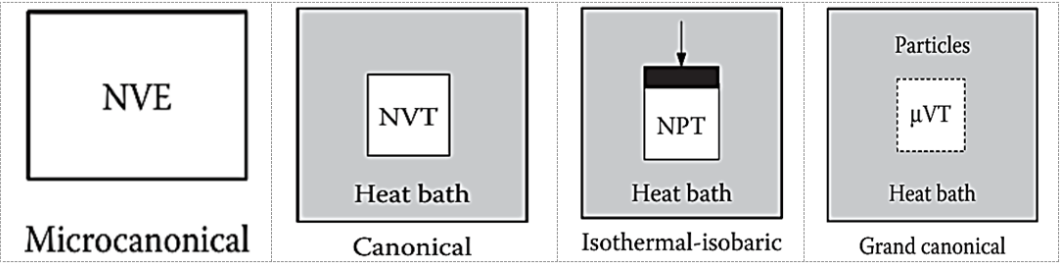

Figure 2: Thermodynamic assembly

Two types of domain boundary temperature control methods can be used: the Andersen thermostat and the Nose-Hoover thermostat. For the Andersen thermostat method **[19],** the system is coupled with a thermostat that imposes the temperature. The Nose-Hoover thermostat method uses a friction term, denoted :

$$m_i\overrightarrow{a_i} = \overrightarrow{f_i} - m_i\zeta\overrightarrow{v_i} \qquad \textbf{Equation (12)}$$

It evolves with the difference between the measured kinetic energy and the desired kinetic energy:

Jilin Daxue Xuebao (Gongxueban)/Journal of Jilin University (Engineering and Technology Edition)
ISSN: 1671-5497
E-Publication: Online Open Access
Vol: 43 Issue: 03-2024
DOI: 10.5281/zenodo.10792464

$$\xi = (E_K - E_K^{Consigne}) / Q_T \qquad \textbf{Equation (13)}$$

Where Q_T determines the speed of thermostat response.

Table 1: thermodynamic assemblies

Ensembles	Independent Variables	Dependent Variables	Z (Partition Function)	Pi (ith state Probability)
Microcanonical	N, V, U	μ, P, T	$\sum_i \delta(E_i - E)$	$\frac{\delta(E_i - E)}{Z_{NVE}}$
Canonical	N, V, T	μ, P, E	$\sum_i e^{-\beta E_i(N,V)}$	$\frac{e^{-\beta E_i(N,V)}}{Z_{NVT}}$
Grand Canonical	V, T, μ	N, P, L	$\sum_i e^{\beta N\mu} Z_{NVT}$	$\frac{e^{-\beta(E_i-\mu N)}}{Z_{NV\mu}}$
Isothermal-Isobaric	N, P, T	μ, V, H	$\sum_i e^{\beta p V_i} Z_{NVT}$	$\frac{e^{-\beta(E-pV_i)}}{Z_{NPT}}$

2.2.4 Point defect diffusion

The diffusion of defects through the solid and the interaction between defects can greatly influence the physical and mechanical properties of the solid, as well as its ageing. When stress is applied to a metal, vacancies can diffuse and form clusters that allow the material to bend, or when the cluster becomes too large, to break.

At the beginning of the 20th century, several complex mechanisms were proposed to explain the diffusion of impurities in solids. These mechanisms, such as direct exchange or ring. However, these mechanisms, illustrated in Figure 3, were quickly ruled out as dominant diffusion mechanisms **[16].** During these processes, a large amount of crystal deformation is involved, creating a significant increase in the energy of the system.

It was then proposed that defects are the main diffusion vectors in crystals. Indeed, atoms and impurities in crystals can exchange places with a gap positioned as the first neighbor. With the site targeted for diffusion unoccupied, activation energy and lattice distortion are reduced, facilitating diffusion. In the case of interstitial defects, a dumbbell diffusion mechanism is preferred.

One of the dumbbell atoms can then push one of its neighbors out of its crystal site in order to share it, while the second atom of the initial dumbbell will take up position in the crystal site that is now no longer shared. The high compactness of metals inhibits the diffusion of atoms through the interstices, unless they are small atoms relative to the size of the interstices.

The substitutional defect will diffuse by either mechanism. A gap near it could cause it to diffuse with a jump to the first neighbor and then return a few moments later to make another jump. It could also pass through a dumbbell mechanism.

Jilin Daxue Xuebao (Gongxueban)/Journal of Jilin University (Engineering and Technology Edition)
ISSN: 1671-5497
E-Publication: Online Open Access
Vol: 43 Issue: 03-2024
DOI: 10.5281/zenodo.10792464

Despite the development of ever more advanced techniques for studying defect diffusion, there are still a number of elements that are not fully understood. Experimental methods can generally provide information on defect diffusion or distribution, but it is difficult to study the underlying mechanism. What's more, these methods have difficulty in studying complex defects such as clusters of lacunae **[17].** Numerical methods, on the other hand, can study the diffusion mechanism and more complex defects, but often have a limited temporal scope. They also depend on costly ab initio calculations to compute the interaction between species, or on potentials, which are less costly, but not always available or optimized for the alloy under study.

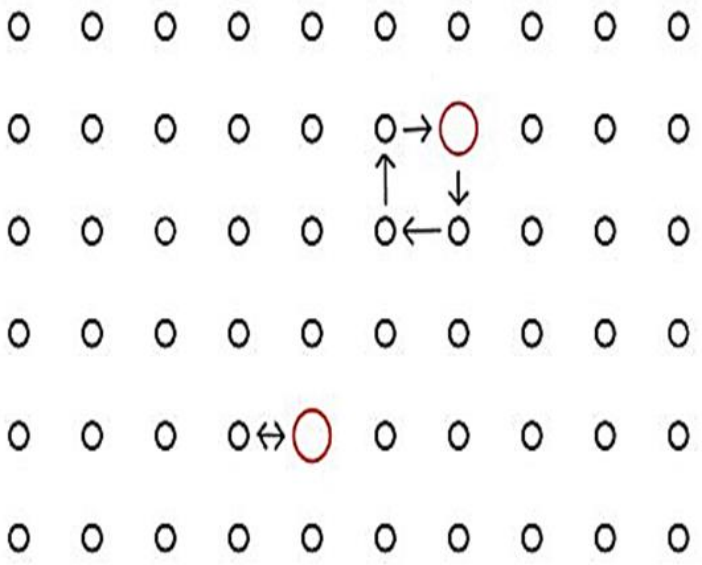

Figure 3: Two mechanisms for the diffusion of impurities (in red) in a crystal presented in the early 1900s. The lower one shows direct exchange and the one at the top of the figure is the ring.

2.2.4.1 Properties of point defects

In order to study and describe the diffusion of point defects in crystals, a number of characteristics are important. These include defect formation energy

The energy of formation of the defect is important in order to know the concentration of the defect in the solid. In many cases, defects may be sufficiently concentrated to have a non-negligible chance of interacting. As a result, the defects could diffuse in groups, and these diffusion mechanisms could become important. In the case of a single-species crystal, the defect formation energy is given by **[18].**

$$E_f = E_N - (N \pm 1 / N) E_{N \pm 1} \qquad \textbf{Equation (14)}$$

Where E_f is the energy of defect formation, E_N is the energy of the perfect crystal, i.e. without defect, N is the number of atoms in the perfect crystal, $E_{N\pm1}$ is the energy of the crystal with defect. The sign in the equation is chosen according to the type of defect. For

Jilin Daxue Xuebao (Gongxueban)/Journal of Jilin University (Engineering and Technology Edition)
ISSN: 1671-5497
E-Publication: Online Open Access
Vol: 43 Issue: 03-2024
DOI: 10.5281/zenodo.10792464

a gap, as one atom is removed from the crystal, the negative sign is chosen. In the case of an interstitial, choose the positive sign.

2.3 Working Procedure

The aim of this study is to provide the vacancy formation energy for different Ti-Al alloys in the BCC phase at operational temperatures 1300,1350,1400 and 1450°K.

To achieve this, a 10x10x10 structure of the TiAl BCC alloy was simulated, with a total of 2000 atoms, in the Large-scale Atomic/Molecular Massively Parallel Simulator (LAMMPS) using a Modified Embedded-Atom Method (MEAM) interatomic potential, and a vacancy was created in the middle of the structure at position (0, 0, 0), reducing the system to 1999 atoms for the final structure.

The energy of the structure before and after vacancy creation was used to determine the energy of vacancy formation.

In addition to calculating the energy of vacancy formation, several different analytical methods were used to determine how vacancy, temperature and alloying affected the overall cohesion of the atomic structure.

We ran a simulation under the LAMMPS version 2020 code with the executable lmp_mpi, under the Windows operating system, using the MEAM potentials found in the database at https://www.ctcms.nist.gov/potentials/system.

Table 2: Additional titanium and nitrogen parameters

elt	atwt	alat	β_0	β_1	β_2	β_3	t_0	t_1	t_2	t_3	esub	asub	α	Z	lat	ibar	rozero
Ti	*47.88*	*2.92*	*2.7*	*1.0*	*3.0*	*1.0*	*1.0*	*6.8*	*-2.0*	*-12.0*	*4.87*	*0.66*	*4.71*	*12*	*hcp*	*3.0*	*1 .0*
Al	*26.98*	*4.04*	*3.20*	*2.6*	*6.0*	*2.6*	*1.0*	*3.05*	*0.51*	*7.75*	*3.36*	*1.16*	*4.68*	*12*	*fcc*	*3.0*	*1.0*

These potentials were used to calculate cohesive energies under different crystallographic structures using the Lammps code and MPC4 software.

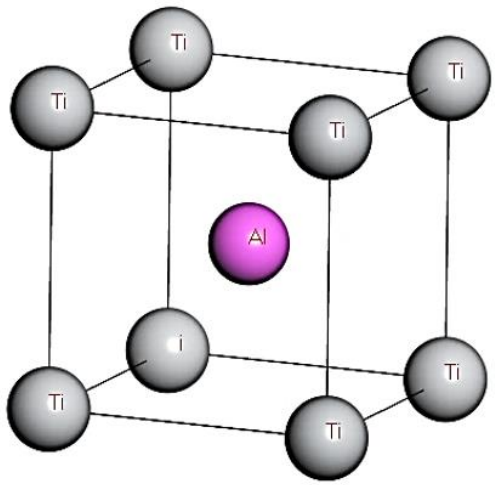

Figure 4: Crystal structure of TiAl alloy in B2 structure

Jilin Daxue Xuebao (Gongxueban)/Journal of Jilin University (Engineering and Technology Edition)
ISSN: 1671-5497
E-Publication: Online Open Access
Vol: 43 Issue: 03-2024
DOI: 10.5281/zenodo.10792464

2.3.1 Molecular dynamics

Molecular dynamics calculation methods use an interatomic potential to correctly simulate the way atoms in a structure interact with each other. In this case, the Modified Embedded-Atom Method (MEAM) was used.

The molecular dynamics code used in this research is LAMMPS (Large-scale Atomic/Molecular Massively Parallel Simulator). The initial configuration consisted of 2000 atoms with periodic boundary conditions in a perfect, unrelaxed BCC lattice. The atoms were then allowed to relax by operating in an isothermal-isobaric ensemble (NPT), where the number of atoms, pressure and temperature were kept constant. Next, the central atom was removed and the remaining 1999 atoms were run in a canonical set (NVT), where the number of atoms, volume and temperature remained constant.

2.3.2 Convergence and averaging of MD time

As we saw earlier, the simulation must first be run long enough for the ensemble-dependent variables to stabilize from the initialized position. Once this has happened, they must also be run long enough to give a statistically valid average. Before and after the removal of the central atom from the lattice structure, the simulation is run for 20 picoseconds with a time step of 1 femtosecond, giving 20,000 steps for each step, and 40,000 steps in total. All properties were averaged over the last 10 picoseconds of each step.

2.3.3 Alloys and structures

Several alloys with different atomic percentages are used here: titanium alloys with 50%, 55% and 60% aluminum. In real life, alloys never have exactly the right atomic percentage. To simulate this phenomenon correctly, the atoms have been **changed at random**.

Starting with a 10x10x10 Ti-Al BCC structure, each atom had a chance to become titanium, this chance being the atomic percentage of aluminum desired in the structure.

2.3.4 Vacancy formation energy

To calculate the vacancy formation energy, a **single vacancy** was introduced into a perfect lattice with equilibrium lattice constants and structural relaxation of atomic positions. Only isolated, non-interacting defects were taken into account when calculating defect formation energy.

In general, the energy of formation of a vacancy in a homogeneous bulk crystal that does not change phase can be described by:

$$E_{fv} = E_{(n-1)} - (n-1/n)\, En \qquad \textbf{Equation (15)}$$

E(n-1) is the total energy of an atomic supercell containing a vacancy, while **En is** the total energy of this supercell before the vacancy was created. In this research, the energy of vacancy formation was calculated by taking averages in two different ways illustrated in the results section.

Jilin Daxue Xuebao (Gongxueban)/Journal of Jilin University (Engineering and Technology Edition)
ISSN: 1671-5497
E-Publication: Online Open Access
Vol: 43 Issue: 03-2024
DOI: 10.5281/zenodo.10792464

1) In this research, vacancy formation energy was calculated by taking averages in three different ways. In the first case, the total energy of the last 10,000 MD steps of each stage was averaged and integrated into equation 3.
2) The energy per atom of each step was then averaged, and these values were used in equation 9. For the error, the variance of the energy per atom of each step was calculated, and these values were then used in equation 10. In the final method, the difference in total energy was calculated for each individual step, as shown in equation 12:

$$E_{v,} = E_{(n-1),\,i} - [(n-1)/n]\, En,_{i} \qquad \textbf{Equation (16)}$$

Next, we calculate the total energy required to create the vacancy:

$$E_v = \Sigma E_v, \quad 10{,}000i = 110{,}000 \qquad \textbf{Equation(17)}$$

3. RESULTS

In this section, we present the results obtained on total energy before and after the creation of the vacancy, the crystalline parameter under the effect of temperature, all these physical quantities for operational temperatures of 1300, 1350, 1400, 1450 and 1500K.

3.1 Total energy and vacancy formation energy

As we saw in the methods section, the vacancy formation energy was calculated using two different methods; both used the total energy of the atomic structure.

As a result, these methods provide incredibly similar results, which are also of the same order of magnitude as previous literature on titanium vacancy formation energy.

The results for total energy before and after vacancy creation are shown in Tables 3 and 4.

3.1.1 Total energies

We present here the results of methods 1 and 2 on total energy in Tables 3 and 4. We note that total energy increases with temperature and decreases with the percentage of aluminum, regardless of the method used.

Table 3: Initial energy method 1

Temperature (K)	Total energy (method 1)		
	%Al		
	50	55	60
1300	-8436.8910	-8552.9930	-8517.2530
1350	-8427.7296	-8536.8788	-8670.3846
1400	-8428.4374	-8529.2554	-8656.4215
1450	-8415.8137	-8523.6181	-8645.8855
1500	-8418.1226	-8517.2530	-8645.9600

Initial energies follow the same (increasing) order, whatever the temperature or percentage of aluminum in the Ti-Al alloy.

Jilin Daxue Xuebao (Gongxueban)/Journal of Jilin University (Engineering and Technology Edition)
ISSN: 1671-5497
E-Publication: Online Open Access
Vol: 43 Issue: 03-2024
DOI: 10.5281/zenodo.10792464

3.1.2 Total final energy and formation energy:

The results of the second method, which are consistent with those of the first, are shown in Table 4. **The formation energy values obtained interpret the possibility of obtaining the structure at any temperature**.

Table 4: Energy of formation (method 2)

Temperature (K)	Formation energy (method 3)								
	%Al								
	50			55			60		
Energy	Ei	Ef	E_f	Ei	Ef	E_f	Ei	Ef	E_f
1300	-8436.8910	-8423.8456	8.8269	-8552.9930	-8553.0975	-4.3809	-8517.2530	-8674.9623	-0.8866
1350	-8427.7296	-8422.1143	1.4014	-8536.8788	-8538.5177	-5.9073	-8670.3846	-8661.0047	5.0447
1400	-8428.4374	-8420.6818	3.5413	-8529.2554	-8532.2200	-7.2292	-8656.4215	-8665.5805	-13.4871
1450	-8415.8137	-8407.3737	4.2321	-8523.6181	-8523.5782	-4.2219	-8645.8855	-8657.4215	-15.8588
1500	-8418.1226	-8405.9762	7.9373	-8517.2530	-8527.1842	-14.1897	-8645.9600	-8640.0599	1.5771

- **For 50%Al:** the structure can form around 1300K and is stable beyond 1450K;
- **For 55%Al:** the structure is quite unstable whatever the operational temperature. This is reflected by the negative formation energies and therefore impossible to form at this percentage;
- **For 60%Al:** the structure presents a duality, it is possible to obtain different (very unstable) phases around 1350 and 1500K.

Total energy is of no significance to vacancy-forming energy.

The results of methods 1 and 2 show that as temperature rises, the structure becomes more stable, especially when the aluminum content reaches 50%.

3.1.3 Energy of formation

The behavior observed on the energy of formation caused by the vacancy revealed by table 4, is almost random for different temperatures but presents a "V" evolution, for the same concentration whose order is translated by high-low-medium energy of formation as we have represented by figure 5.

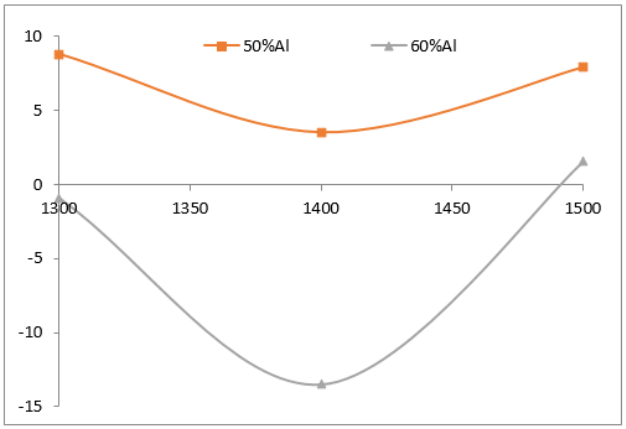

Figure 5: Energy of formation method 3

Jilin Daxue Xuebao (Gongxueban)/Journal of Jilin University (Engineering and Technology Edition)
ISSN: 1671-5497
E-Publication: Online Open Access
Vol: 43 Issue: 03-2024
DOI: 10.5281/zenodo.10792464

Figure 5 shows that, whatever the temperature, the Ti-50%Al structure remains possible, unlike the others, and 60%Al, which show stability at the lower and upper extremes respectively. Above 1400°K, however, the 60%Al structure is stable.

3.2 Influence of temperature on the mesh parameter

We have monitored the mesh parameter behavior of each of these titanium alloys, the results of which are presented in Table 5, where the variation of the crystalline parameter has been of key interest.

Table 5: Mesh parameter evolution by temperature and %Al

Temperature (K)	Temperature and parameter								
	%Al								
	50			55			60		
	init	final	diff	init	final	diff	init	final	diff
1300	**32.7**	**32.6968**	**-0.0032**	32.7	**32.6981**	**-0.0019**	32.7	**32.6992**	**-0.0008**
1350	**32.7**	**32.6975**	**-0.0025**	32.7	**32.6988**	**-0.0012**	**32.7**	**32.6996**	**-0.0004**
1400	**32.7**	**32.6983**	**-0.0017**	32.7	**32.6993**	**-0.0007**	32.7	**32.7008**	**0.0008**
1450	**32.7**	**32.6988**	**-0.0012**	32.7	**32.7001**	**0.0001**	32.7	**32.7013**	**0.0013**
1500	**32.7**	**32.6995**	**-0.0005**	32.7	**32.7007**	**0.0007**	32.7	**32.7020**	**0.0020**

- **For 50%Al:** although the difference decreases with temperature, it decreases negligibly, proving that the structure is stable around 50%Al;
- **For 60%Al:** this structure shows the opposite tendency to the 50%Al structure, a particular phenomenon is reported which can be interpreted by the growth of the lattice parameter, observed around 1450K. However, we cannot affirm that this phenomenon is consistent with the presence of the gap in the 60%Al structure.

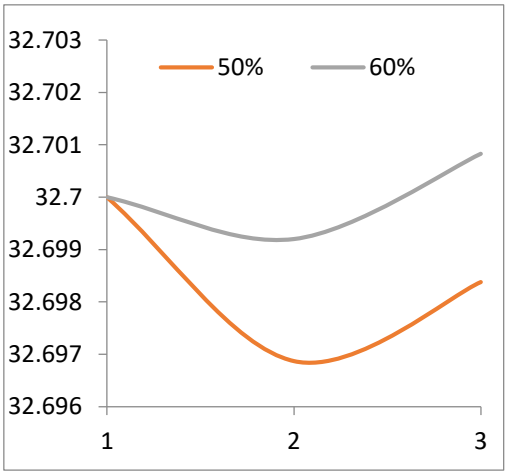

Figure 6 a) : Mesh parameter by Temperature

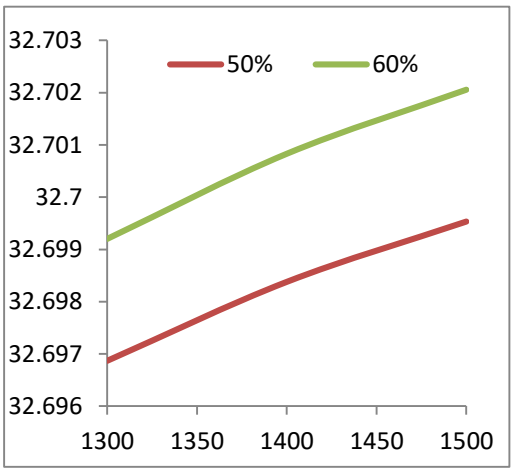

Figure 6 b) : b): Mesh parameter for %Al

Figure 6 shows that, at the same temperatures, the difference in the crystalline parameter decreases with the percentage, and the higher the percentage, the less the structure deforms.

Jilin Daxue Xuebao (Gongxueban)/Journal of Jilin University (Engineering and Technology Edition)
ISSN: 1671-5497
E-Publication: Online Open Access
Vol: 43 Issue: 03-2024
DOI: 10.5281/zenodo.10792464

3.2.1 Crystalline parameter

We have plotted the crystalline parameter as a function of pitch to analyze the structure's behavior, and found that the final structures do not have the same parameters (see Table 5).

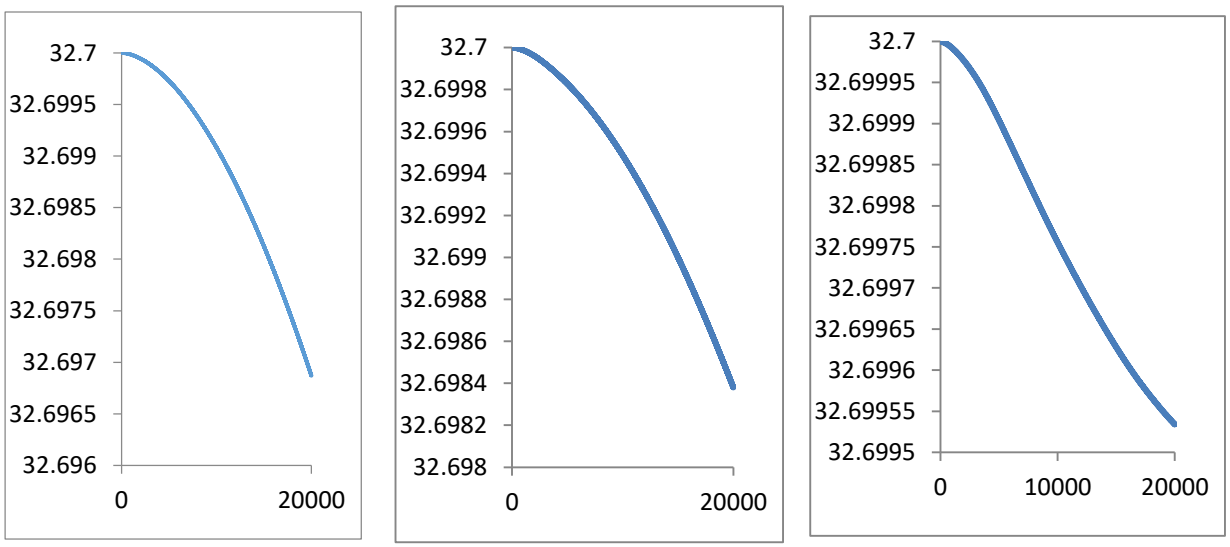

Figure 7 a): parameter curve for 50%Al

For 50%Al: the trend is identical for operating temperatures below 1500K, at which temperature the evolution of the parameter becomes linear.

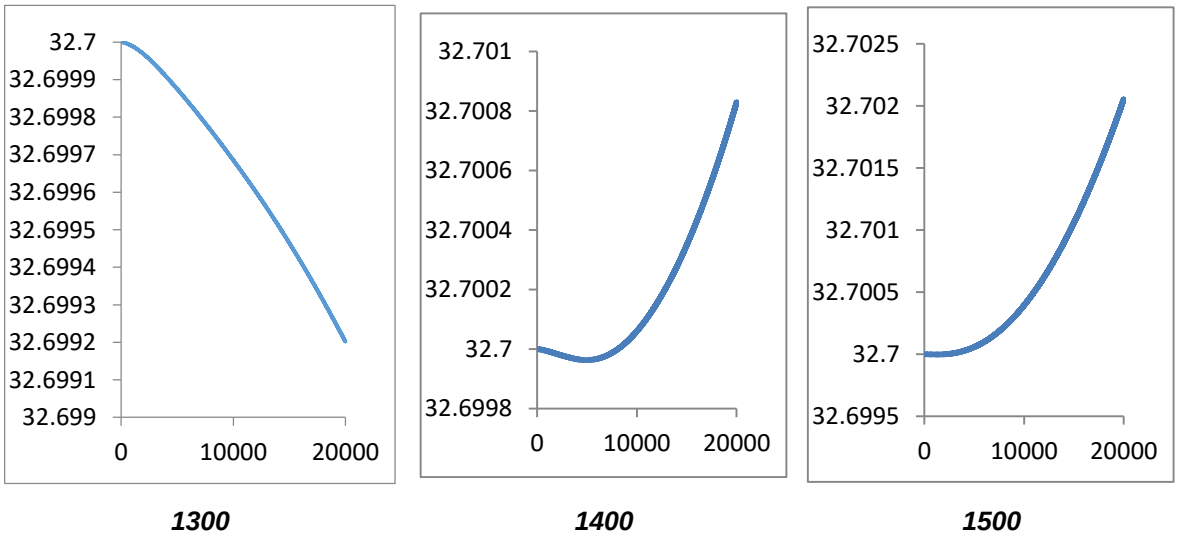

Figure 7 b): Parameter curve for 60%Al

For 60%Al: the curve is very distinctive, starting out linear and then curving in the opposite direction to other alloys, above 1350K.

Jilin Daxue Xuebao (Gongxueban)/Journal of Jilin University (Engineering and Technology Edition)
ISSN: 1671-5497
E-Publication: Online Open Access
Vol: 43 Issue: 03-2024
DOI: 10.5281/zenodo.10792464

We observed a reversal in the evolution of the lattice parameter around 1350K, and this observation was closely followed on the NPT and NVT assemblies represented by figure 8 below for Ti-60%Al.

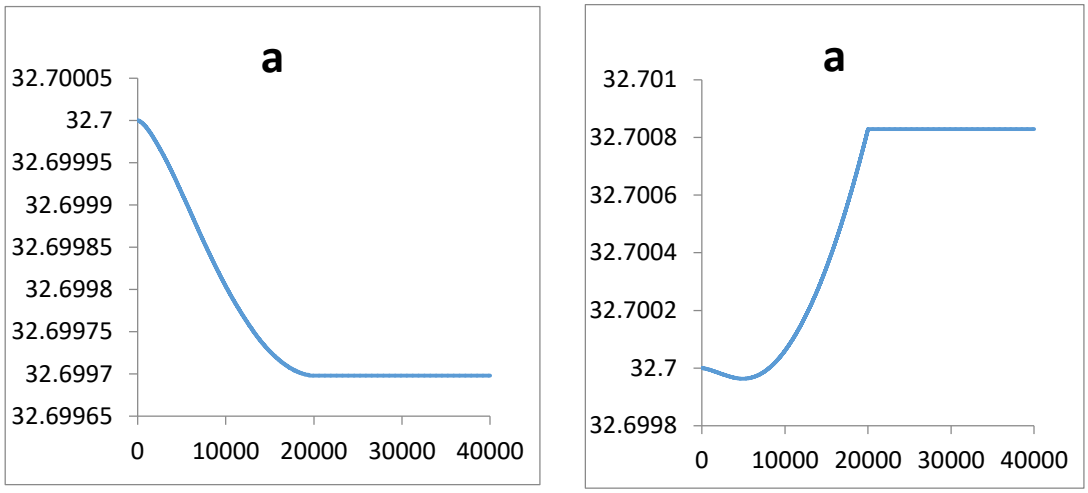

Figure 8 :Mesh parameter trends (NPT+ NVT assemblies) 60%Al at 1350 and 1400K

This reversal in the evolution of the lattice parameter can result in a phase change around / beyond 1350K.

However, we have observed the behavior of the mesh energy around these points, as shown in figure 9 below:

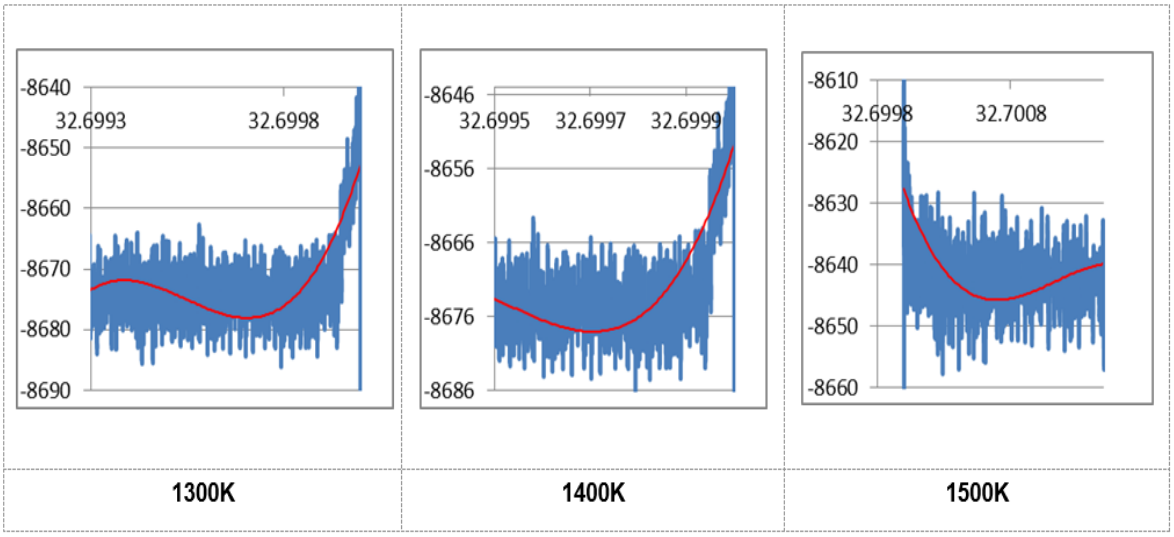

Figure 9: Polynomial trend energy vs. crystal parameter for 60%Al

Jilin Daxue Xuebao (Gongxueban)/Journal of Jilin University (Engineering and Technology Edition)
ISSN: 1671-5497
E-Publication: Online Open Access
Vol: 43 Issue: 03-2024
DOI: 10.5281/zenodo.10792464

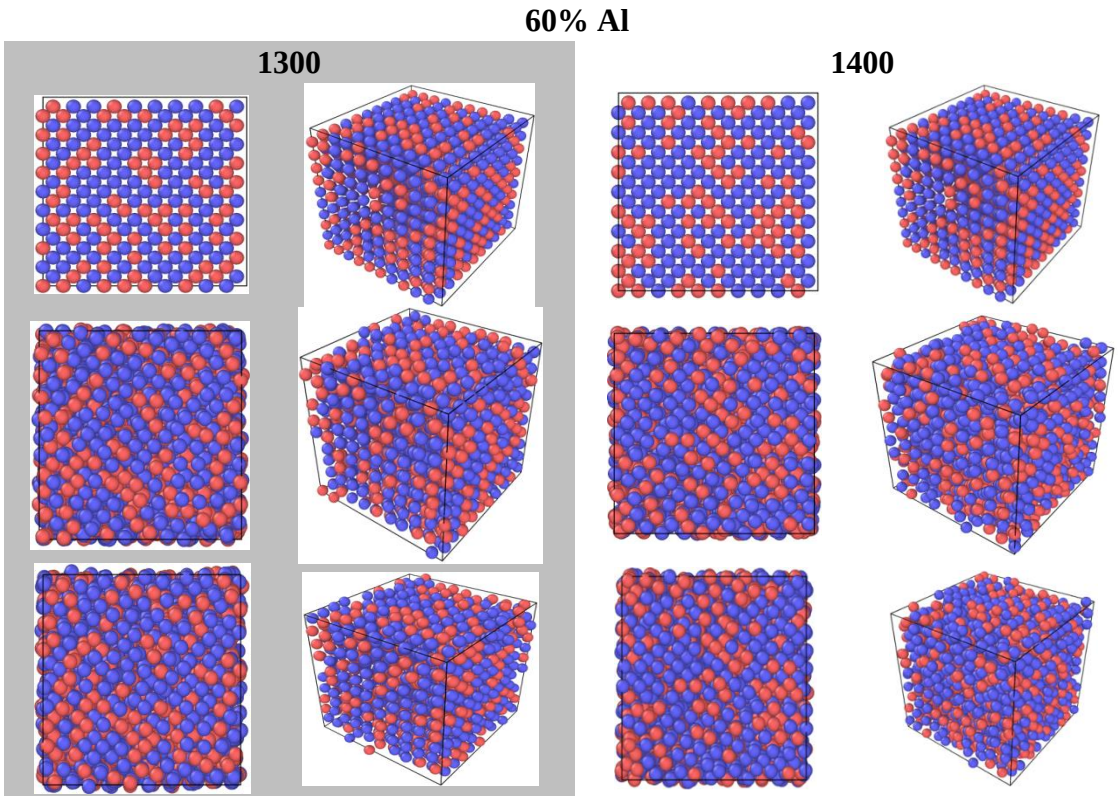

Figure 10: Mesh evolution initial, intermediate and final phases / front view and perspective for 60%Al, 1300 and 1400K

4. GENERAL CONCLUSION AND OUTLOOK

In the course of this work, we used the LAMMPS calculation code based on molecular dynamics. This work produced good results by employing the MEAM potentials of Ti and Al and also TiAl found in the database, without which observation of the vacant site effect would have been impossible.

We have shown that for selected operating temperatures, the Ti-x%Al structure exhibits different behavior at temperatures of 1350K and 1400K. The Ti-50Al alloy has positive formation energies, so this structure forms at selected operating temperatures, which is not the case for Ti-55%Al. At 1350K, we observed a reversal in the mesh parameter behavior of the Ti-60%Al alloy, which we attributed to the phase change around 1350K.

At 1400K, we observed a reversal in the behavior of total energy.In short, around 1400K, there are many alloys close to Ti-60%Al with the same energy, caused by the insertion of the vacant site.

However, it would be interesting to continue this study around temperatures 1350-1400K and 1400-1500K for the 60%Al alloy. In the future, it would be interesting to study the phenomenon resulting from particle diffusion, as well as filling rates in Ti-60%Al alloys.

Jilin Daxue Xuebao (Gongxueban)/Journal of Jilin University (Engineering and Technology Edition)
ISSN: 1671-5497
E-Publication: Online Open Access
Vol: 43 Issue: 03-2024
DOI: 10.5281/zenodo.10792464

Bibliographical References

1) J. DUPUIS, Investigation d'alliages à base de titane de types béta-métastables pour applications marines: cas particulier d'un winch innovant, PhD thesis, Rennes, 2014, p.1.

2) S. AMELIO, Évolution microstructurale d'un alliage a base TiAl. sollicitation mécanique par compression dynamique et stabilité thermique, PhD thesis, Lorraine,2005, p.1.

3) Y. COMBRES, Metallurgy and recycling of titanium and its alloys, Techniques de l'Ingénieur, ME3 M2355, 06/1997.

4) Military handbook titanium and titanium alloys. MIL-DBK-697 A, 1974.

5) C. BECQUART and M. PEREZ. Molecular dynamics applied to materials. Techniques de l'ing'enieur, RE136, (2010).

6) L. Verlet, Phys. Rev. B 159, 98 (1967).

7) S. Koonin and D. Meredith, Computational Physics (Perseus Books, 1990), fortran edition ed.

8) S. Nosé, J. Chem. Phys. 81, 7182 (1984).

9) S. Nosé, Mol. Phys. 57, 187 (1986).

10) H. Andersen, J. Chem. Phys. 72, 2384 (1980).

11) M.Parrinello and A. Rahman, J. Appl. Phys. 52, 7182 (1981).

12) J. L. Murray, Calculation of the Titanium-Aluminium Phase Diagram, Metallurgical Transactions A 19A (1988) 243

13) J. J. Valencia, C. McCullough, C. G. Levi, R. Mehrabian, Microstructure evolution during conventional and rapid solidification of a Ti-50 at. % Al alloy, Scripta Metallurgica 21 (1987) 1341

14) C. McCullough, J. J. Valencia, H. Mateos, C. G. Levi, R. Mehrabian, K. A. Rhyne, The high temperature α field in the Titanium-Aluminium phase diagram, Scripta Metallurgica 22 (1988) 1131

15) C. McCullough, J. J. Valencia, C. G. Levi, R. Mehrabian, Phase equilibria and solidification in Ti-Al alloys, Acta Metallurgica 37 (1989) 1321

16) S. C. Huang, P. A. Siemers, Characterization of the high-temperature phase fields near stoichiometric γ-TiAl, Metallurgical Transactions A 20A (1989) 1899

17) E. L. Hall, S. C. Huang, Microstructures of rapidly-solidified binary TiAl alloys, Acta Metallurgica et Materialia 38 (1990) 539

18) Helmut Mehrer. Diffusion Mechanism, pages 94-104. Springer, 2007.

19) Filip Tuomisto and Ilja Makkonen. Defect identification in semiconductors with positron annihilation: Experiment and theory. Rev. Mod. Phys. 85:1583-1631, Nov 2013.

20) Sami Mahmoud, Mickaël Trochet, Oscar A. Restrepo, and Normand Mousseau. Study of point defects diffusion in nickel using kinetic activation-relaxation technique. Acta Materialia, 144:679 - 690, 2018.

21) R. TRICOT, Thermo-mechanical Treatments of Titanium Alloys, Proc. 6th World Conf. On Titanium, Cannes, France, June 1988.

22) J. L. Murray, Al-Ti (Aluminium-Titanium), A. T. B. Massalski, Serie: Binary Alloy Phase Diagrams 2 (1986) 173